Structure, Volume *22*

Supplemental Information

Lytic Water Dynamics Reveal Evolutionarily Conserved Mechanisms of ATP Hydrolysis by TIP49 AAA+ ATPases

Arina Afanasyeva, Angela Hirtreiter, Anne Schreiber, Dina Grohmann, Georgii Pobegalov, Adam R. McKay, Irina Tsaneva, Michael Petukhov, Emmanuel Käs, Mikhail Grigoriev, and Finn Werner

Supplemental Figure S1 (related to Figure 1). Amino-acid sequence alignment and important features of archaeal and eukaryotic TIP49 proteins. ClustalW alignment of two archaeal TIP49 proteins (mk, *Methanopyrus kandleri*; pa, *Pyrococcus abyssi*) and two eukaryotic TIP49a and TIP49b proteins (hs, *Homo sapiens*; sc, *Saccaromyces cerevisae*). The residues highlighted in blue represent the Walker A and B, Sensor I and II and the R-finger motifs. Domain boundaries are indicated by black (D1), red (D2) and green (D3) colors. The OB-fold and L2 loop are delineated by brackets and the FCR tri-peptide insertion corresponding to the *lik*TIP49b mutation is indicated with an arrow.

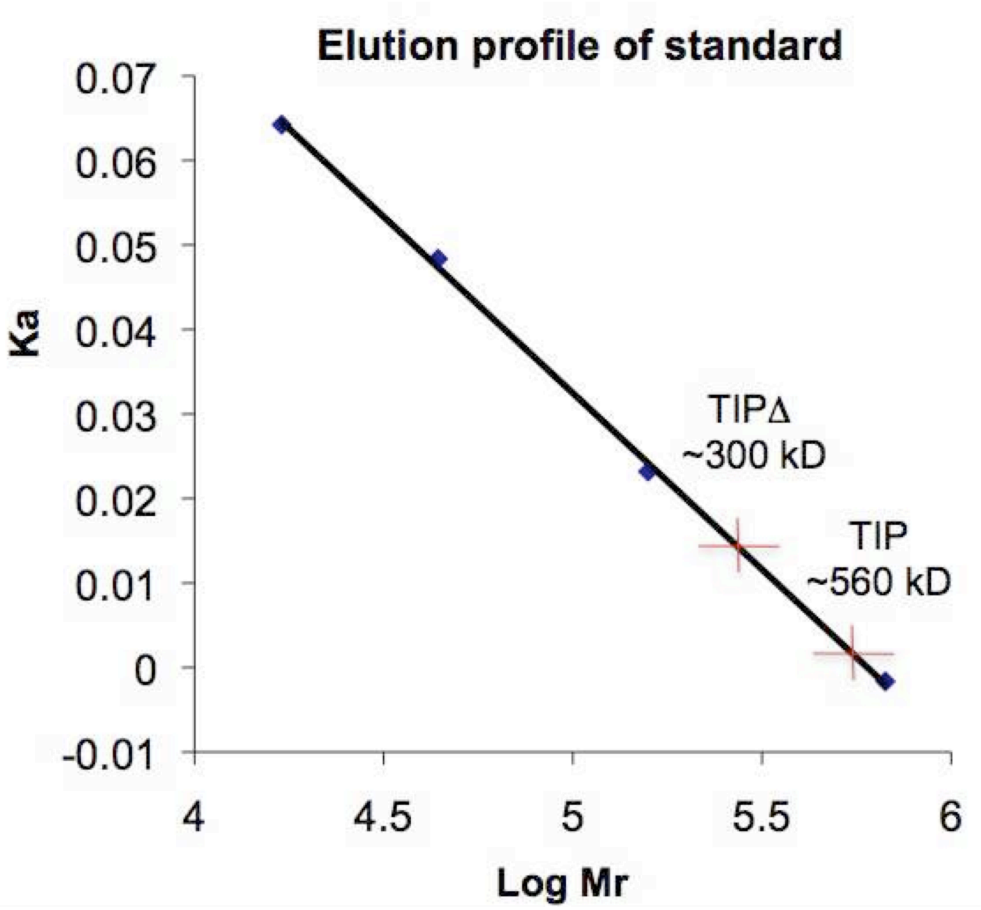

Supplemental Figure S2 (related to Figures 3 and 4). Calibration of the Superdex 200 column (GE Healthcare) with size standards (Bio-Rad laboratories). The four markers cover a range from 17 to 670 kDa and the elution volumes of mkTIP49 and TIPΔD2 correspond to approximate molecular weights of 560 and 300 kDa respectively.

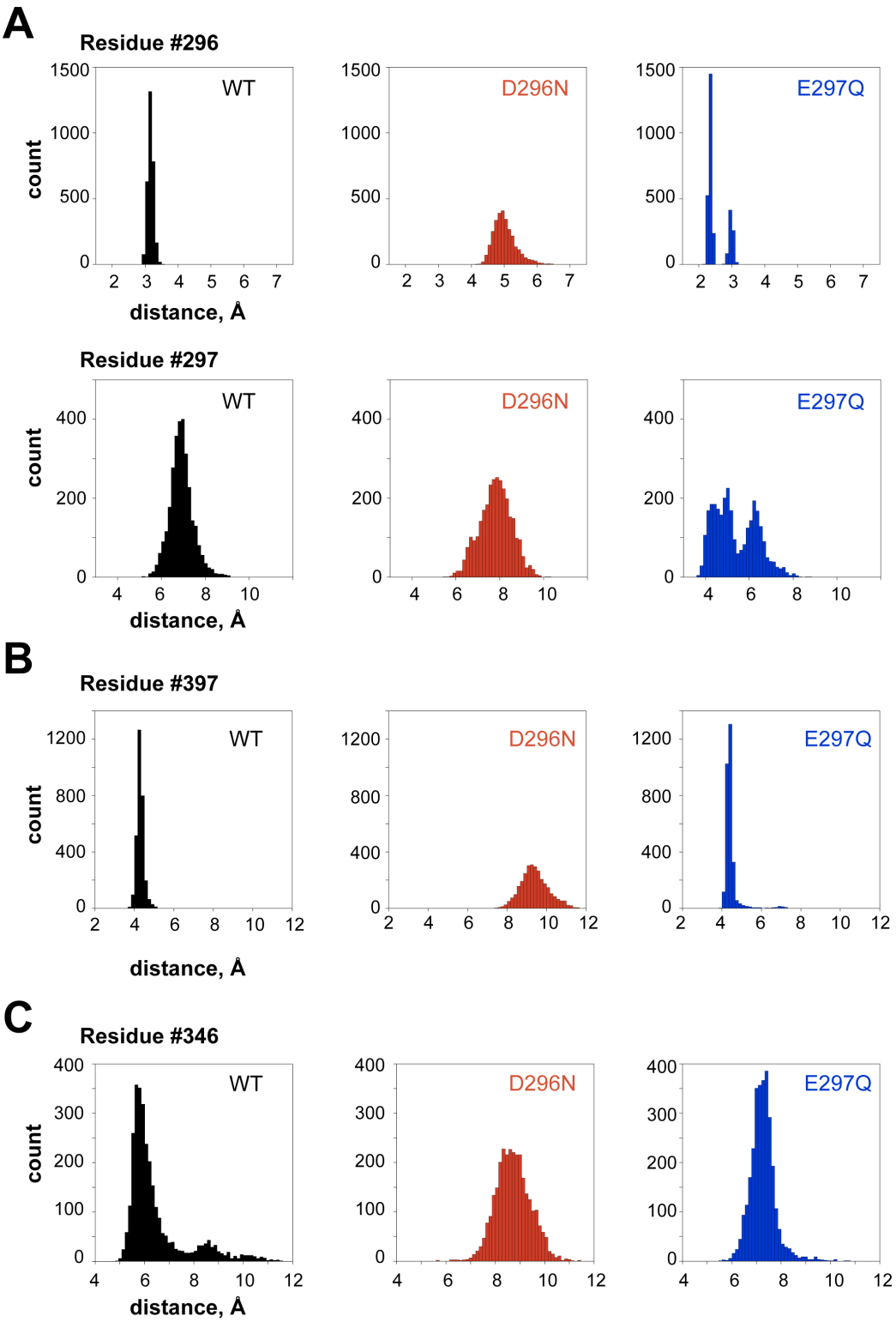

Supplemental Figure S3 (related to Figure 4). **A**. Distribution of distances between $C\gamma_{296}$ or $C\delta_{297}$ and Mg^{2+} in the wild type (black), D296N (red) and E297Q (blue) proteins. **B**. Distribution of distances between the guanidyl group of R397 and Pγ. **C**. the distribution for the $C\gamma_{346}$-Pγ is shown. Distances were calculated as described in the online Experimental Procedures section.

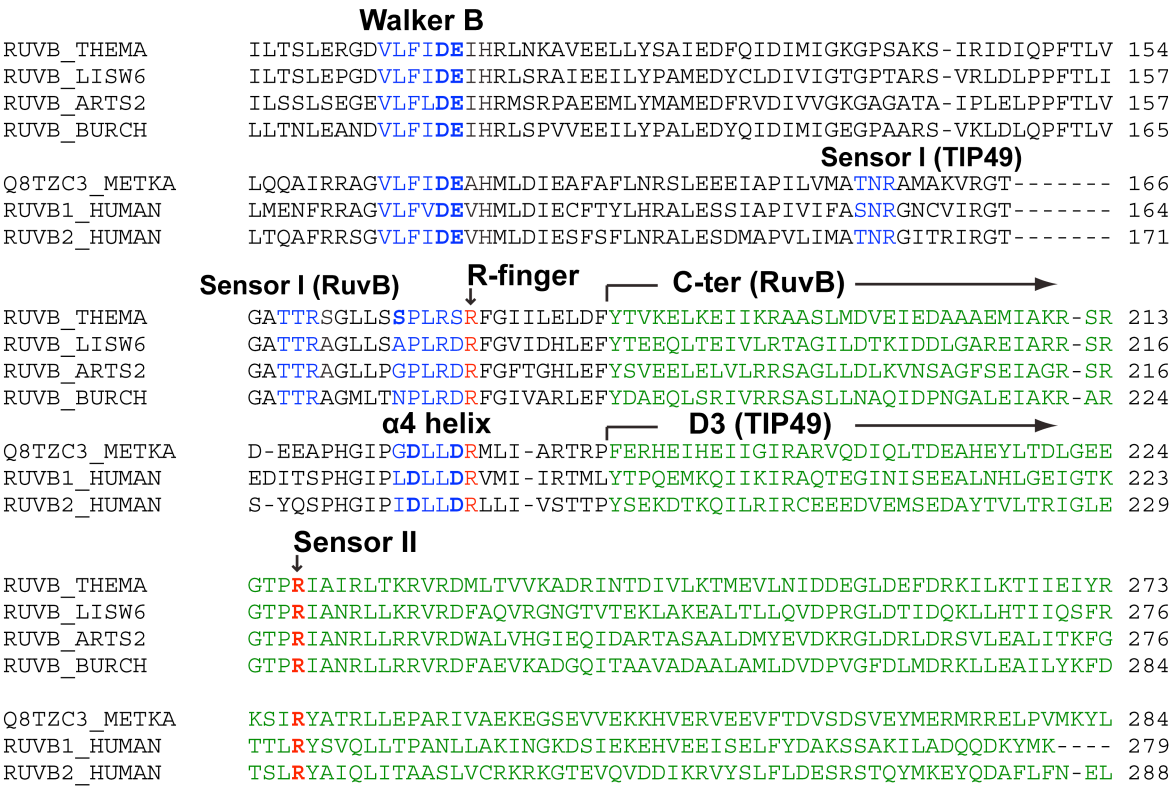

Supplemental Figure S4 (related to Figure 7). ClustalW alignment of the amino-acid sequences of archaeal D2-deleted mkTIP49 (Q8TZC3_METKA), human TIP49 proteins (RUVB1_HUMAN and RUVB2_HUMAN), and RuvB proteins (RUVB_THEMA, RUVB_LISW6, RUVB_ARTS2 and RUVB_BURCH). Only partial sequences under study are shown for the sake of simplicity.

Online Experimental Procedures

Modeling and MD simulations

Molecular modeling was performed as described (Petukhov et al., 2012). Molecular dynamic (MD) simulations of mkTIP49 using the GROMACS 4.5.5 software package on the multiprocessor clusters of the St. Petersburg State Polytechnical University and of the "Kurchatov Institute" National Research Centre (Moscow) were performed as described in (Petukhov et al., 2012; Van Der Spoel et al., 2005). The calculations of the drift distances of the mkTIP49 domains (taken as the mass centers of distinct atomic groups) and of the Cα-RMSD values were performed using the *g_dist* and *g_rms* utilities, respectively, as implemented in the GROMACS software package, using the MD trajectories as input files.

Accessibility of ATP to attacking water molecules was calculated as the cumulative probability (denoted as P_w) of water occupancy in the minimal volume situated in front of the γ-phosphate group. This volume, accommodating one water molecule at a time, was defined as a sphere with 1.4-Å radius that corresponds to the dimensions of a water molecule, and was placed at a distance of 2.5 Å from the γ-phosphate group. P_w was calculated as the fraction of time when the water molecule is present in this volume. Because ATP hydrolysis requires the activation of a water molecule by neighboring proton-accepting residues (Grigorenko et al., 2011; Senior et al., 2002), we also calculated the probability of H-bond formation between the lytic water molecule, located in the appropriate position in front of the γ-phosphate group of ATP, and the negatively charged residues that may act as proton acceptors (*i.e.* E297, D346 and D349 of mkTIP49). For calculations of “appropriate” water positions, H-bond length and the distance to each putative proton-accepting residue were set to 1.8-2.1 Å. The donor α_1 angle between the donor H-O group of water and the acceptor oxygen from the side-chain carbonyl groups was varied from 150° to 180°. The side-chain acceptor α_2 angle formed between the side-chain carbonyl groups and the water proton was varied from 90° to 180° (Finkelstein and Ptitsyn, 2002). All distances and angles were

calculated using the atomic coordinates recorded at each 10-ps time step of the 30-ns MD simulations.

Cloning and recombinant protein expression and purification

Methanopyrus kandleri genomic DNA was isolated from cell pellets (a gift from the University of Regensburg) using DNAeasy kits (Qiagen). The gene encoding mkTIP49 (locus tag MK0007) was cloned by PCR amplification from genomic DNA. The resulting TIP49 fragment was cloned into the pET21a(+) expression vector, using NdeI/BamHI restriction sites to generate constructs encoding untagged recombinant proteins. To simplify the purification procedures, N-terminally His-tagged mkTIP49 variants were generated by cloning mkTIP49 fragments into the pET151D-TOPO vector (Invitrogen). The domain boundaries of the archaeal TIP49 were identified by amino-acid sequence and structure alignments (Gorynia et al., 2011; Petukhov et al., 2012; Putnam et al., 2001). The full-length TIP49 sequence spans residues 1-456, and the TIPΔD2 variant residues 1-142 fused in frame to residues 291-456. The TIP insertion domain (residues 143-290) was cloned into pGEX-2TK using BamHI restrictions sites to generate an N-terminal GST-fusion protein (Putnam et al., 2001). A second TIP insertion-domain variant including 19 additional N-terminal amino acids encompassing residues 124-290 (Matias et al., 2006) was cloned into pET151D-TOPO to generate an N-terminal His-tagged fusion protein. Recombinant expression vectors were transformed into competent BL21 [DE3] Rosetta2 cells (Novagen). The resulting expression strains were grown and expanded in Terrific Broth and induced with 1 mM IPTG for 4 hours at 37 ˚C after reaching an A_{600} of ~0.8. The bacterial cells were collected by centrifugation (6000 rpm for 10') and soluble proteins were extracted in NPI-20 buffer (0.3 M NaCl, 50 mM Na_xPO_4 pH 8.0, 20 mM imidazole) in the presence of lysozyme (1 mg/ml, Sigma), RNaseA (20 mg/ml, Roche Biochemicals) and Turbo-DNase (1 U/ml, Amicon) and repeated sonication. His-tagged proteins were metal affinity-purified on a BioLogic DuoFlow chromatography system (Bio-Rad Laboratories) using a 1-ml HisTrap cartridge (GE

Healthcare), NPI-20 wash buffer and NPI-250 elution buffer (0.3 M NaCl, 50 mM Na_xPO_4 pH 8.0, 250 mM imidazole). The GST-TIP insertion-domain fusion protein was purified on a 5 ml GST-Trap cartridge (GE Healthcare) and eluted with 5 mM glutathione. The GST-tag was cleaved with Thrombin (1 u/ml) overnight at 4 ˚C and the GST fusion tag removed by heat treatment at 75 ˚C for 20'. All recombinant proteins were dialyzed against P300 (300 mM Potassium acetate, 20 mM Tris-acetate pH 7.9, 10 mM Magnesium acetate, 10 % glycerol, 10 mM beta-Mercaptoethanol) or N1000 buffer (1000 mM NaCl, 20 mM Tris-acetate pH 7.9, 10 mM Magnesium acetate, 10 % glycerol, 10 mM beta-Mercaptoethanol).

Untagged recombinant TIP49 proteins were purified by heat treatment (incubation at 75°C for 20') and insoluble material was removed by centrifugation at 14,000 rpm for 20'. Size exclusion chromatography was carried out on Superdex 200 and Superose 6 columns (GE Healthcare) using a flow rate of 0.5 ml/min in either P300 or N1000 buffer on a BioLogic DuoFlow chromatography system (Bio-Rad laboratories). Denaturating SDS PAGE was carried out using Laemmli buffers and Protean III gel systems (Bio-Rad). Native gel electrophoresis was carried out using ready-cast 4-12 % Tris-Glycine gels (Novex/Invitrogen) with Tris-Glycine running buffer.

mkTIP49 mutagenesis

Single mutations were generated in the mkTIP49 expression plasmid (pET151D-TOPO- mkTIP) by site-directed mutagenesis (QuikChange® II site-directed mutagenesis kit). Mutagenic primers were incorporated by changing AAC to GTT at position N326Q and GAT to AAC at position D346N. Expression and purification of the mutant proteins were performed exactly as for the wild-type protein, as described above. Protein concentrations were measured with the Qubit© Protein assay kit using a Qubit© 2.0 fluorometer (Introgen™). Size exclusion chromatography of the various mkTIP proteins was performed on Superose™ 6 10/30 GL column (GE Healthcare).

ATPase assays

For wild-type or mutant mkTIP49, ATPase reactions were carried out at 75 ºC for 30' in a total volume of 100 µl using 1-4 µl TIP49 protein and 1 mM ATP in 1.5 M potassium acetate, 50 mM Tris-acetate, pH 8, 25 mM Mg-acetate, 0.5 mM EDTA, and 0.1 mM DTT. ATP hydrolysis was measured by phosphate released in a malachite green-based chromogenic assay (PiColorLock™ ALS, Innova Biosciences). The absorbance at 635 nm was measured in 96-well plates in a Labtech LT4000 microplate reader. The specific activity was calculated as mol ATP hydrolyzed/mol TIP49 protein over 30'.

Nanoelectrospray ionization mass spectrometry

Recombinant mkTIP49 proteins were buffer-exchanged into 250 mM ammonium acetate at pH 7.5 by FPLC on a Superdex 200 10/300 gel filtration column fitted to an AKTA purification system (GE Healthcare, Piscataway, NJ, USA). FPLC fractions were pooled and concentrated using Vivaspin 2ml centrifugal concentrators with a molecular weight cut-off of 10 kDa (Sartorius, Aubagne, France). Ions were generated by nanoelectrospray ionization and spectra acquired on an LCT Premier XE mass spectrometer (Waters, Manchester, UK) modified for high-mass operation. Nitrogen gas was leaked into the initial stages of the vacuum chamber to aid the radial focusing of high-mass ions (Chernushevich and Thomson, 2004). Typically, nanospray ionization was performed using 2-3 µl of aqueous protein solution and a capillary voltage of 1.6-1.9 kV. Ion-transfer stage pressures of 1.5×10^{-3} - 2.0×10^{-2} mbar were required. External calibration was achieved by using a 33 mg/ml aqueous solution of cesium iodide (Sigma, St. Louis, MO, USA).

Supplemental References

Chernushevich, I.V., and Thomson, B.A. (2004). Collisional cooling of large ions in electrospray mass spectrometry. Anal Chem 76, 1754-1760.

Finkelstein, A.P., and Ptitsyn, O.B. (2002). Protein physics: a course lecture (London, San Diego: Academic Press, Elsevier Science).

Gorynia, S., Bandeiras, T.M., Pinho, F.G., McVey, C.E., Vonrhein, C., Round, A., Svergun, D.I., Donner, P., Matias, P.M., and Carrondo, M.A. (2011). Structural and functional insights into a dodecameric molecular machine - the RuvBL1/RuvBL2 complex. Journal of structural biology 176, 279-291.

Grigorenko, B.L., Kaliman, I.A., and Nemukhin, A.V. (2011). Minimum energy reaction profiles for ATP hydrolysis in myosin. Journal of molecular graphics & modelling 31, 1-4.

Matias, P.M., Gorynia, S., Donner, P., and Carrondo, M.A. (2006). Crystal structure of the human AAA+ protein RuvBL1. The Journal of biological chemistry 281, 38918-38929.

Petukhov, M., Dagkessamanskaja, A., Bommer, M., Barrett, T., Tsaneva, I., Yakimov, A., Queval, R., Shvetsov, A., Khodorkovskiy, M., Käs, E., *et al.* (2012). Large-scale conformational flexibility determines the properties of AAA+ TIP49 ATPases. Structure 20, 1321-1331.

Putnam, C.D., Clancy, S.B., Tsuruta, H., Gonzalez, S., Wetmur, J.G., and Tainer, J.A. (2001). Structure and mechanism of the RuvB Holliday junction branch migration motor. Journal of molecular biology 311, 297-310.

Senior, A.E., Nadanaciva, S., and Weber, J. (2002). The molecular mechanism of ATP synthesis by F1F0-ATP synthase. Biochimica et biophysica acta 1553, 188-211.

Van Der Spoel, D., Lindahl, E., Hess, B., Groenhof, G., Mark, A.E., and Berendsen, H.J. (2005). GROMACS: fast, flexible, and free. J Comput Chem 26, 1701-1718.